

Highly efficient triarylene conjugated dyes for sensitized solar cells†

Yuan Jay Chang^a and Tahsin J. Chow^{*b}

Received 8th January 2011, Accepted 28th February 2011

DOI: 10.1039/c1jm10107b

A new series of organic dyes containing a triarylamine donor group, a triarylene-linked bridging moiety, and a cyanoacrylic acid acceptor group were synthesized through a simple procedure in high yields. A selected set of substituents were added onto the phenyl group *ortho* to the cyanoacrylic acid in order to examine their influences on the performance of dye-sensitized solar cells (DSSCs). Their photochemical behaviors were examined under AM1.5 solar condition (100 mW cm⁻²). A typical device made with a compound containing a -CF₃ substituent (**PSP-CF₃**) displayed a short-circuit current (J_{sc}) 15.16 mA cm⁻², an open-circuit voltage (V_{oc}) 0.68 V, a fill factor (ff) 0.68, corresponding to an overall conversion efficiency of 7.0% and a maximal monochromatic incident photon-to-current conversion efficiency (IPCE) 78%. Their photophysical and electrochemical properties were analyzed with the aid of a time-dependent density functional theory (TDDFT) model with the B3LYP functional. Their HOMO and LUMO energy levels are verified by both electrochemical measurements and theoretical calculations.

Introduction

Dye-sensitized solar cells (DSSCs) have been considered as a promising alternative energy source.¹ The ruthenium-based complexes, *i.e.*, N3, N719, and black dye reported by Michael Grätzel, have achieved maximal power conversion efficiencies over 11%.² Compared with metallic materials, organic dyes are indispensable due to their advantages of environmental friendliness, higher structural flexibility, lower cost, easier preparation and purification, *etc.* A wide variety of organic dyes have been reported in the literature including the derivatives of coumarin,³ indoline,⁴ cyanine,⁵ merocyanine,⁶ hemicyanine,⁷ perylene,⁸ dithienylsilole,⁹ and porphyrin,¹⁰ *etc.*, whilst most of them exhibited energy-to-electricity conversion efficiency in a range 5~9%. In our previous studies we have developed a series of organic dipolar dyes composed of an aromatic amine donor (D) and a cyanoacrylic acid acceptor (A), which were separated by a linearly connected phenylene-thiophenylene-phenylene bridge (PSP). The performance of DSSCs made with these dyes can achieve a maximal quantum efficiency of 7%, considerably close to that of N719.¹¹ To further improve their performance and also to investigate their structure/performance relationship, certain

selected substitutions on their triarylene bridge are made.¹² Five new organic dyes, *i.e.*, **PSP-H**, **PSP-F**, **PSP-CN**, **PSP-CF₃** and **PSP-OCH₃** (Chart 1) were synthesized in this regard. The tuning of electron flow by the addition of a substituent can be viewed from two sides, *i.e.*, the presence of an electron-withdrawing group located on the acceptor side can stabilize the charge-separated excited state; whilst an electron-donating group may improve the charge injection efficiency toward the TiO₂ conducting electrode. Nevertheless, the absorption wavelength will be red-shifted with respect to the parent structure, as a result of more extended electronic resonance induced by the substituents. A broader absorption range reveals that more photons can be harvested by DSSCs.¹³ In all the five structures, the central thiophenylene moiety is replaced by a 3,4-ethylenedioxythiophylene (EDOT) group in order to enhance the absorbance of the dyes.^{14,15} Their device characteristics made with these dyes are examined in this report.

Experimental

General information

All reactions and manipulations were carried out under a nitrogen atmosphere. Solvents were distilled freshly according to standard procedures. ¹H and ¹³C NMR spectra were recorded on Bruker (AV 400/AV 500 MHz) spectrometer in CDCl₃, THF-*d*₈, and DMSO-*d*₆ as a solvent. Chemical shifts are reported in δ scale downfield from the peak for tetramethylsilane. Absorption spectra were recorded on a Jasco-550 spectrophotometer. Emission spectra and photoluminescence quantum yield were obtained from a Hitachi F-4500 spectrofluorimeter. The emission spectra in solutions were measured in spectral grade solvent

^aDepartment of Chemistry, National Taiwan University, No.1, Sec. 4, Roosevelt Rd., Da'an Dist., Taipei, 10617, Taiwan. E-mail: d93223006@ntu.edu.tw; Fax: +886-2-27884179; Tel: +886-2-27898641

^bInstitute of Chemistry, Academia Sinica, No.128, Sec. 2, Academia Rd., Nangang Dist., Taipei, 11529, Taiwan. E-mail: tjchow@chem.sinica.edu.tw; Fax: +886-2-27884179; Tel: +886-2-27898552

† Electronic Supplementary Information (ESI) available: ¹H and ¹³C NMR, infrared, and EIS spectra. Experimental for the synthesis of 1. TDDFT simulated data. Loading amount of the dyes. See DOI: 10.1039/c1jm10107b/

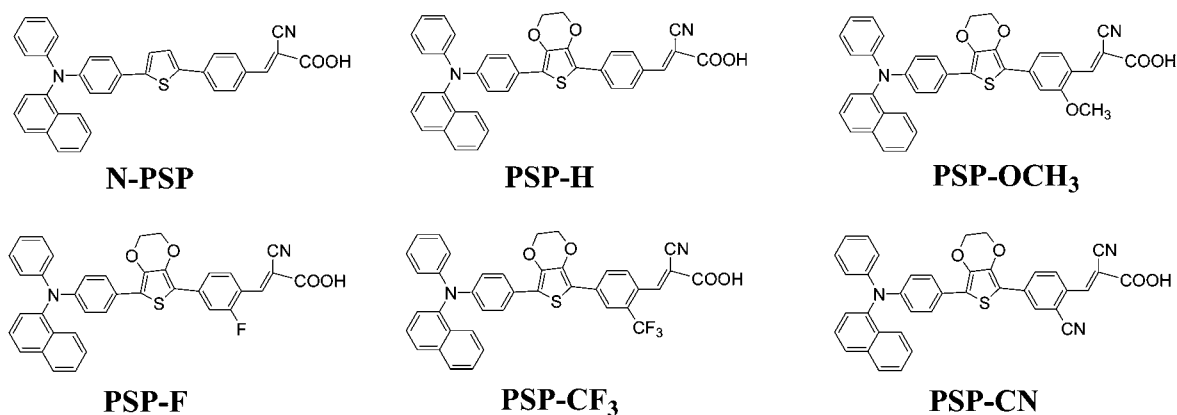


Chart 1 The structures of organic dyes.

by a 90° angle detection, and those of thin film were recorded by front-face detection. The redox potentials were measured by using cyclic voltammetry on a CHI 620 analyzer. All measurements were carried out in THF solutions containing 0.1 M tetrabutylammonium hexafluorophosphate (TBAPF₆) as supporting electrolyte at ambient condition after purging 10 min with N₂. The conventional three electrode configuration was employed, which consists of a glassy carbon working electrode, a platinum counter electrode, and a Ag/Ag⁺ reference electrode calibrated with ferrocene/ferrocenium (Fc/Fc⁺) as an internal reference. Mass spectra were recorded on a VG70-250S mass spectrometer.

All chemicals, *i.e.*, *o*-tolunitrile, 1,4-dibromo-2-fluorobenzene, 4-bromo-2-methoxyphenylmethanol, *n*-butyllithium (1.6 M in hexane), *trans*-dichlorobis(triphenylphosphine) palladium(II), *N,N*-dimethylformamide, sulfuric acid, nitric acid, zinc powder, *N*-bromosuccinimide, trimethylamine *N*-oxide, pyridinium chlorochromate, cyanoacetic acid, ammonium acetate, and triethyl amine, were purchased from ACROS, Merck, Lancaster, TCI, Sigma-Aldrich, separately, and purified while necessary before use. The synthetic procedures of compound **1** is shown in ESI. Chromatographic separations were carried out by using silica gel from Merck, Kieselgel si 60 (40–63 μm).

Fabrication and characterization of DSSCs

The FTO conducting glass (FTO glass, fluorine doped tin oxide over-layer, transmission <90% in the visible, sheet resistance 8 Ω square⁻¹), titania-oxide pastes of Ti-Nanoxide T/SP and Ti-Nanoxide R/SP were purchased from Solaronix. A thin film of TiO₂ (16~18 μm thick) was coated on a 0.25 cm² FTO glass substrate. It was immersed in a THF solution containing 3 × 10⁻⁴ M dye sensitizers for at least 12 h, then rinsed with anhydrous acetonitrile and dried. Another piece of FTO with sputtering 100 nm thick Pt was used as a counter electrode. The active area was controlled at a dimension of 0.25 cm² by adhering a 60 μm thick polyester tape on the Pt electrode. The photocathode was placed on top of the counter electrode and was tightly clipped together to form a cell. Electrolyte was then injected into the seam between two electrodes. An acetonitrile solution containing LiI (0.5 M), I₂ (0.05 M) and 4-*tert*-butylpyridine (0.5 M) was used as the electrolyte. Devices made of

a commercial dye N719 under the same condition (3 × 10⁻⁴ M, Solaronix S.A., Switzerland) was used as a reference. The cell parameters were obtained under an incident light with intensity 100 mW cm⁻² measured by a thermopile probe (Oriol 71964), which was generated by a 300 W Xe lamp (Oriol 6258) passing through a AM 1.5 filter (Oriol 81088). The current–voltage parameters of DSSCs were recorded by a potentiostat/galvanostat model CHI650B (CH Instruments, USA). The light intensity was further calibrated by an Oriol reference solar cell (Oriol 91150) and adjusted to be 1.0 sun. The monochromatic quantum efficiency was recorded through a monochromator (Oriol 74100) at short circuit condition.

4-Bromo-2-trifluoromethylbenzaldehyde (2)

To a solution of 1,4-dibromo-2-trifluoromethylbenzene (5 g, 19.85 mmol) in THF at –78 °C was added dropwise *n*-BuLi (12.4 mL, 19.85 mmol, 1.6 M in hexane). The mixture was stirred for 1 h, then to it was added DMF (2.3 mL, 29.78 mmol). The reaction was stirred with a magnetic bar for 1 h, then was quenched by adding water and extracted with ethyl acetate. The organic layer was dried over anhydrous MgSO₄ and evaporated under vacuum. The products were purified by silica gel column chromatograph eluted with dichloromethane–hexane (1/9). A colorless liquid of **2** was obtained in 40% yield (2.0 g, 7.94 mmol). Spectroscopic data of **2**: δ_H (400 MHz, CDCl₃) 10.36 (s, 1H), 8.02 (d, 1H, *J* = 8.4 Hz), 7.96 (s, 1H), 7.88 (d, 1H, *J* = 8.4 Hz); δ_C (100 MHz, CDCl₃) 187.6, 135.6, 132.3, 130.5, 129.4, 128.7, 124.1, 121.3; *m/z* (FAB) 251.9392 (M⁺, C₈H₄BrF₃O requires 251.9398).

4-Bromo-2-methoxybenzaldehyde (3)

A mixture of 4-bromo-2-methoxyphenylmethanol (2.00 g, 9.21 mmol) and pyridinium chlorochromate (1.97 g, 9.21 mmol) in dry CH₂Cl₂ was stirred with a magnetic bar for 4 h. The reaction was quenched by adding water, and then was extracted with dichloromethane. The organic layer was dried over anhydrous MgSO₄ and evaporated under vacuum. The products were purified by silica gel column chromatograph eluted with dichloromethane–hexane (1/1). White solids of **3** were obtained in 92% yield (1.81 g, 8.47 mmol). Spectroscopic data of **3**: δ_H (400 MHz, CDCl₃) 10.38 (s, 1H), 7.67 (d, 1H, *J* = 8.0 Hz), 7.17 (d, 1H, *J* = 8.4 Hz), 7.15 (d, 1H, *J* = 1.6 Hz); δ_C (100 MHz,

CDCl₃) 188.7, 161.9, 130.5, 129.7, 124.2, 123.7, 115.3, 56.0; *m/z* (EI) 213.9634 (M⁺, C₈H₇BrO₂ requires 213.9629).

***p*-(5-(*p*-(Naphthylphenylamino)phenyl)-3,4-ethylenedioxythiophen-2-yl)benzaldehyde (4-H)**

To a mixture of 4-bromobenzaldehyde (1.22 g, 6.60 mmol), PdCl₂(PPh₃)₂ (139 mg, 0.20 mmol), and 2-tributylstannyl-5-(*p*-(naphthylphenylamino)phenyl)-3,4-ethylenedioxythiophene (7.18 g, 9.9 mmol) in a three-necked flask was added DMF (20 mL). The mixture was stirred at 90 °C for 24 h. After cooling, the reaction was quenched by adding MeOH and saturated KF (15 mL). It was extracted with CH₂Cl₂ and the organic layer dried over anhydrous MgSO₄. Evaporation of the solvent gave a crude product, which was purified by silica gel with hexane as the eluent. The orange solid of **4-H** was obtained in 78% yield (2.77 g, 5.15 mmol). Spectroscopic data for **4-H**: δ_H (400 MHz, CDCl₃) 9.96 (s, 1H), 7.97 (d, 1H, *J* = 8.4 Hz), 7.93–7.84 (m, 5H), 7.81 (d, 1H, *J* = 8.4 Hz), 7.61 (d, 2H, *J* = 8.8 Hz), 7.52–7.47 (m, 2H), 7.40 (d, 1H, *J* = 9.6 Hz), 7.38 (d, 1H, *J* = 7.2 Hz), 7.28–7.23 (m, 2H), 7.13 (d, 2H, *J* = 8.0 Hz), 7.03 (d, 2H, *J* = 8.8 Hz), 6.99 (d, 1H, *J* = 7.6 Hz), 4.39–4.37 (m, 2H), 4.34–4.32 (m, 2H); δ_C (100 MHz, CDCl₃) 191.4, 147.9, 147.5, 143.1, 140.7, 139.3, 137.8, 135.3, 133.7, 131.2, 130.1, 129.2, 128.4, 127.3, 127.1, 126.7, 126.5, 126.3, 126.2, 125.6, 125.4, 124.1, 122.5, 122.3, 121.1, 118.5, 112.7, 64.7, 64.4; *m/z* (FAB) 540.1644 ((M + H)⁺, C₃₅H₂₅NO₃S requires 540.1633).

4-(5-(*p*-(Naphthylphenylamino)phenyl)-3,4-ethylenedioxythiophen-2-yl)-2-fluorobenzaldehyde (4-F)

Compound **4-F** was synthesized according to a similar procedure as that of **4-H**, giving orange solids of **4-F** in 60% yield. δ_H (400 MHz, CDCl₃) 10.3 (s, 1H), 7.96 (d, 1H, *J* = 8.4 Hz), 7.92 (d, 1H, *J* = 8.0 Hz), 7.96 (d, 1H, *J* = 8.4 Hz), 7.84 (d, 1H, *J* = 8.4 Hz), 7.82 (d, 1H, *J* = 8.0 Hz), 7.64–7.47 (m, 6H), 7.39 (t, 1H, *J* = 6.8 Hz), 7.38 (d, 1H, *J* = 7.6 Hz), 7.28–7.23 (m, 2H), 7.13 (d, 1H, *J* = 7.6 Hz), 7.04–6.99 (m, 3H), 4.41–4.39 (m, 2H), 4.35–4.33 (m, 2H); δ_C (100 MHz, CDCl₃) 187.0, 166.2, 163.7, 147.8, 143.0, 141.5, 141.4, 137.7, 135.3, 131.2, 129.2, 129.1, 128.8, 128.4, 127.3, 127.2, 126.8, 126.5, 126.3, 126.2, 125.0, 124.3, 124.1, 122.6, 122.4, 122.0, 121.8, 121.6, 121.3, 121.2, 121.1, 120.9, 119.5, 64.8, 64.3; *m/z* (FAB) 557.1458 (M⁺, C₃₅H₂₄FNO₃S requires 557.1461).

4-(5-(*p*-(Naphthylphenylamino)phenyl)-3,4-ethylenedioxythiophen-2-yl)-2-cyanobenzaldehyde (4-CN)

Compound **4-CN** was synthesized according to the same procedure as that of **4-H**, giving orange solids of **4-CN** in 58% yield. δ_H (400 MHz, CDCl₃) 10.3 (s, 1H), 8.24 (s, 1H), 7.94–7.89 (m, 4H), 7.80 (d, 1H, *J* = 8.4 Hz), 7.57 (d, 2H, *J* = 8.4 Hz), 7.50–7.45 (m, 2H), 7.37 (t, 1H, *J* = 8.0 Hz), 7.35 (d, 1H, *J* = 7.6 Hz), 7.23 (t, 2H, *J* = 8.0 Hz), 7.11 (d, 2H, *J* = 7.6 Hz), 7.01–6.97 (m, 3H), 4.46–4.44 (m, 2H), 4.38–4.36 (m, 2H); δ_C (100 MHz, CDCl₃) 187.4, 148.0, 147.6, 142.9, 142.1, 139.6, 137.8, 135.3, 133.0, 131.1, 130.2, 129.8, 129.2, 126.8, 126.5, 126.3, 126.2, 124.6, 124.0, 122.7, 122.6, 120.7, 116.3, 114.4, 110.3, 64.9, 64.3; *m/z* (FAB) 564.1506 (M⁺, C₃₆H₂₄N₂O₃S requires 564.1508).

4-(5-(*p*-(Naphthylphenylamino)phenyl)-3,4-ethylenedioxythiophen-2-yl)-2-(trifluoromethyl)benzaldehyde (4-CF₃)

Compound **4-CF₃** was synthesized according to the same procedure as that of **4-H**, giving orange solids of **4-CF₃** in 55% yield. δ_H (400 MHz, CDCl₃) 10.3 (s, 1H), 8.16 (s, 1H), 8.11 (d, 1H, *J* = 8.4 Hz), 7.96 (t, 2H, *J* = 8.4 Hz), 7.92 (d, 1H, *J* = 8.4 Hz), 7.82 (d, 1H, *J* = 8.4 Hz), 7.61 (d, 2H, *J* = 8.8 Hz), 7.53–7.47 (m, 2H), 7.39 (t, 1H, *J* = 8.4 Hz), 7.37 (d, 1H, *J* = 7.6 Hz), 7.28–7.23 (m, 2H), 7.13 (d, 2H, *J* = 8.0 Hz), 7.03–6.99 (m, 3H), 4.40–4.38 (m, 2H), 4.33–4.31 (m, 2H); δ_C NMR (100 MHz, CDCl₃) 188.2, 147.8, 147.7, 142.9, 141.6, 138.8, 137.8, 135.3, 131.6, 131.3, 131.1, 130.1, 129.5, 129.2, 128.4, 127.8, 127.3, 127.2, 126.8, 126.5, 126.3, 126.2, 125.1, 124.9, 124.1, 122.6, 122.4, 120.8, 119.7, 111.4, 64.8, 64.3; *m/z* (FAB) 607.1428 (M⁺, C₃₆H₂₄F₃NO₃S requires 607.1429).

4-(5-(*p*-(Naphthylphenylamino)phenyl)-3,4-ethylenedioxythiophen-2-yl)-2-methoxybenzaldehyde (4-OCH₃)

Compound **4-OCH₃** was synthesized according to the same procedure as that of **4-H**, giving orange solids of **4-OCH₃** in 75% yield. δ_H (400 MHz, CDCl₃) 10.45 (s, 1H), 8.00 (d, 1H, *J* = 8.4 Hz), 7.92 (d, 1H, *J* = 8.0 Hz), 7.82 (t, 1H, *J* = 8.0 Hz), 7.63 (d, 2H, *J* = 8.8 Hz), 7.52–7.47 (m, 2H), 7.42–7.38 (m, 4H), 7.26 (t, 2H, *J* = 7.2 Hz), 7.15 (d, 2H, *J* = 7.6 Hz), 7.06–6.99 (m, 2H), 4.35–4.34 (m, 2H), 4.30–4.29 (m, 2H); δ_C (100 MHz, CDCl₃) 188.8, 162.0, 147.9, 147.6, 143.1, 140.8, 140.7, 137.8, 135.3, 131.2, 129.2, 128.8, 128.5, 127.3, 127.1, 126.8, 126.5, 126.4, 126.2, 125.4, 124.1, 122.5, 122.4, 122.3, 121.1, 118.4, 117.9, 113.0, 108.1, 64.8, 64.3; *m/z* (FAB) 569.1666 (M⁺, C₃₆H₂₇NO₄S requires 569.1661).

(*E*)-2-(4-(5-(*p*-(Naphthylphenylamino)phenyl)-3,4-ethylenedioxythiophen-2-yl)phenyl)cyanoacrylic acid (PSP-H)

A mixture of **4-H** (1 g, 1.85 mmol), cyanoacetic acid (189 mg, 2.22 mmol), and ammonium acetate (36 mg, 0.46 mmol) in acetic acid was placed in a three-necked flask under a nitrogen atmosphere and was stirred at 120 °C for 12 h. After cooling, the reaction was quenched by adding water, then was extracted with CH₂Cl₂. The organic layer was dried over anhydrous MgSO₄ and evaporated under vacuum. The products were purified by silica gel column chromatograph eluted with CH₂Cl₂/acetic acid (19/1). The deeply red solid was isolated in 72% yield (807 mg, 1.33 mmol), mp: 293–295 °C. Spectroscopic data of **PSP-H**: δ_H (400 MHz, DMSO-*d*₆) 8.21 (s, 1H), 8.02 (d, 3H, *J* = 8.0 Hz), 7.92 (d, 1H, *J* = 8.4 Hz), 7.82 (d, 3H, *J* = 8.4 Hz), 7.60–7.50 (m, 4H), 7.43 (d, 1H, *J* = 8.0 Hz), 7.26 (t, 2H, *J* = 8.0 Hz), 7.00 (d, 3H, *J* = 8.0 Hz), 6.99 (d, 2H, *J* = 8.8 Hz), 4.42 (d, 2H, *J* = 3.6 Hz), 4.35 (d, 2H, *J* = 3.6 Hz); δ_C (100 MHz, DMSO-*d*₆) 163.9, 153.2, 147.6, 147.5, 142.7, 141.7, 138.6, 137.4, 135.4, 131.8, 130.9, 129.9, 129.5, 129.1, 127.7, 127.4, 127.2, 127.1, 126.8, 125.6, 125.2, 123.7, 123.0, 122.5, 120.9, 117.4, 117.1, 112.1, 103.1, 65.3, 64.8; *m/z* (FAB) 607.1699 ((M + H)⁺, C₃₈H₂₆N₂O₄S requires 607.1691).

(*E*)-2-(4-(5-(*p*-(Naphthylphenylamino)phenyl)-3,4-ethylenedioxythiophen-2-yl)-2-fluorophenyl)cyanoacrylic acid (PSP-F)

Compound **PSP-F** was synthesized according to the same procedure as that of **PSP-H**, giving black solids of **PSP-F** in

53% yield, mp: 261~263 °C. δ_{H} (400 MHz, THF- d_6) 8.47 (t, 1H, $J = 8.4$ Hz), 8.44 (s, 1H), 7.95 (d, 2H, $J = 7.6$ Hz), 7.85 (d, 1H, $J = 8.4$ Hz), 7.71 (d, 2H, $J = 8.8$ Hz), 7.64 (d, 2H, $J = 8.8$ Hz), 7.52 (t, 1H, $J = 8.0$ Hz), 7.48 (t, 1H, $J = 7.6$ Hz), 7.38 (t, 2H, $J = 8.8$ Hz), 7.23 (t, 2H, $J = 7.6$ Hz), 7.11 (d, 2H, $J = 8.0$ Hz), 6.99–6.97 (m, 3H), 4.47 (d, 2H, $J = 3.6$ Hz), 4.39 (d, 2H, $J = 3.6$ Hz); δ_{C} (100 MHz, THF- d_6) 164.4, 161.8, 149.0, 148.9, 144.2, 143.2, 139.4, 136.6, 132.3, 130.1, 129.88, 129.4, 128.2, 127.7, 127.3, 127.2, 127.1, 126.5, 125.0, 123.6, 123.4, 122.2, 121.8, 112.6, 112.3, 66.1, 65.5; m/z (FAB) 625.1605 ((M + H)⁺, C₃₈H₂₅FN₂O₄S requires 625.1597).

(E)-2-(4-(5-(p-(Naphthylphenylamino)phenyl)-3,4-ethylenedioxythiophen-2-yl)cyanophenyl)cianoacrylic acid (PSP-CN)

A mixture of 4-CN (0.8 g, 1.42 mmol), cyanoacetic acid (145 mg, 1.70 mmol), and excess triethylamine in toluene was placed in a three-necked flask under a nitrogen atmosphere and was stirred at 120 °C for 12 h. After cooling, the reaction was quenched by adding water, then was extracted with CH₂Cl₂. The organic layer was dried over anhydrous MgSO₄ and evaporated under vacuum. The products were purified by silica gel column chromatography eluted with CH₂Cl₂/acetic acid (19/1). The black solids of PSP-CN were isolated in 10% yield (89 mg, 0.14 mmol), mp: 212~214 °C. Spectroscopic data of PSP-CN: δ_{H} (400 MHz, DMSO- d_6) 8.26 (d, 1H, $J = 8.4$ Hz), 8.21 (s, 1H), 8.13 (s, 1H), 8.00 (d, 1H, $J = 8.4$ Hz), 7.97 (d, 1H, $J = 8.4$ Hz), 7.91 (d, 1H, $J = 8.4$ Hz), 7.82 (d, 1H, $J = 8.4$ Hz), 7.59–7.49 (m, 4H), 7.42 (t, 1H, $J = 7.6$ Hz), 7.35 (d, 1H, $J = 7.2$ Hz), 7.26 (t, 2H, $J = 7.6$ Hz), 7.01–6.97 (m, 3H), 6.87 (d, 2H, $J = 8.8$ Hz), 4.44 (d, 2H, $J = 3.2$ Hz), 4.34 (d, 2H, $J = 3.2$ Hz); δ_{C} (100 MHz, DMSO- d_6) 163.3, 147.6, 147.5, 143.3, 142.6, 142.1, 138.5, 135.8, 135.4, 132.4, 130.9, 129.9, 129.4, 129.2, 129.1, 128.9, 127.7, 127.4, 127.2, 127.1, 126.8, 125.0, 123.7, 123.0, 122.6, 120.8, 118.2, 118.0, 117.2, 114.0, 110.2, 65.4, 64.8; m/z (FAB) 632.1654 ((M + H)⁺, C₃₉H₂₅N₃O₄S requires 632.1643).

(E)-2-(4-(5-(p-(Naphthylphenylamino)phenyl)-3,4-ethylenedioxythiophen-2-yl)-2-(trifluoromethyl)phenyl)cianoacrylic acid (PSP-CF₃)

Compound PSP-CF₃ was synthesized according to the same procedure as that of PSP-H, giving black solids of PSP-CF₃ in 55% yield, mp: 269~271 °C. δ_{H} (400 MHz, DMSO- d_6) 8.43 (s, 1H), 8.14 (d, 1H, $J = 8.4$ Hz), 8.10 (s, 1H), 7.99 (d, 1H, $J = 8.0$ Hz), 7.96 (d, 1H, $J = 8.8$ Hz), 7.90 (d, 1H, $J = 8.4$ Hz), 7.81 (d, 1H, $J = 8.4$ Hz), 7.58–7.48 (m, 4H), 7.41 (t, 1H, $J = 8.0$ Hz), 7.35 (d, 1H, $J = 7.2$ Hz), 7.25 (t, 2H, $J = 7.6$ Hz), 7.01–6.97 (m, 3H), 6.87 (d, 2H, $J = 8.8$ Hz), 4.43 (d, 2H, $J = 3.6$ Hz), 4.34 (d, 2H, $J = 3.6$ Hz). δ_{C} (100 MHz, DMSO- d_6) 162.9, 162.9, 148.6, 147.7, 147.5, 142.6, 142.2, 138.5, 136.6, 135.4, 131.2, 130.9, 129.9, 129.0, 128.8, 128.4, 127.7, 127.4, 127.2, 127.1, 126.8, 125.2, 124.9, 123.7, 123.1, 122.7, 122.5, 120.7, 118.2, 115.9, 110.6, 109.3, 65.4, 64.7. m/z (FAB) 675.1571 ((M + H)⁺, C₃₉H₂₅F₃N₂O₄S requires 675.1564).

(E)-2-(4-(5-(p-(Naphthylphenylamino)phenyl)-3,4-ethylenedioxythiophen-2-yl)-2-methoxyphenyl)cianoacrylic acid (PSP-OCH₃)

Compound PSP-OCH₃ was synthesized according to the same procedure as that of PSP-H, giving black solids of PSP-OCH₃ in 70% yield, mp: 294~296 °C. δ_{H} (400 MHz, DMSO- d_6) 8.42 (s, 1H), 8.09 (d, 1H, $J = 8.4$ Hz), 7.96 (d, 1H, $J = 8.0$ Hz), 7.86 (d, 1H, $J = 8.0$ Hz), 7.78 (d, 1H, $J = 8.4$ Hz), 7.51 (t, 1H, $J = 7.2$ Hz), 7.46 (d, 3H, $J = 7.6$ Hz), 7.37 (t, 1H, $J = 7.2$ Hz), 7.29 (d, 3H, $J = 7.2$ Hz), 7.21 (t, 2H, $J = 7.2$ Hz), 6.95 (d, 3H, $J = 7.2$ Hz), 6.81 (d, 2H, $J = 8.0$ Hz), 4.35 (d, 2H, $J = 3.6$ Hz), 4.28 (d, 2H, $J = 3.6$ Hz), 3.85 (s, 3H); δ_{C} NMR (100 MHz, DMSO- d_6) 164.3, 159.4, 147.5, 147.4, 146.7, 142.7, 141.7, 139.4, 138.5, 135.3, 130.9, 129.8, 129.0, 127.6, 127.3, 127.2, 127.1, 126.8, 125.2, 123.7, 122.9, 122.5, 120.8, 118.2, 117.7, 117.5, 117.4, 112.3, 107.7, 102.2, 65.2, 64.7, 56.2; m/z (FAB) 637.1806 ((M + H)⁺, C₃₉H₂₈N₂O₅S requires 637.1797).

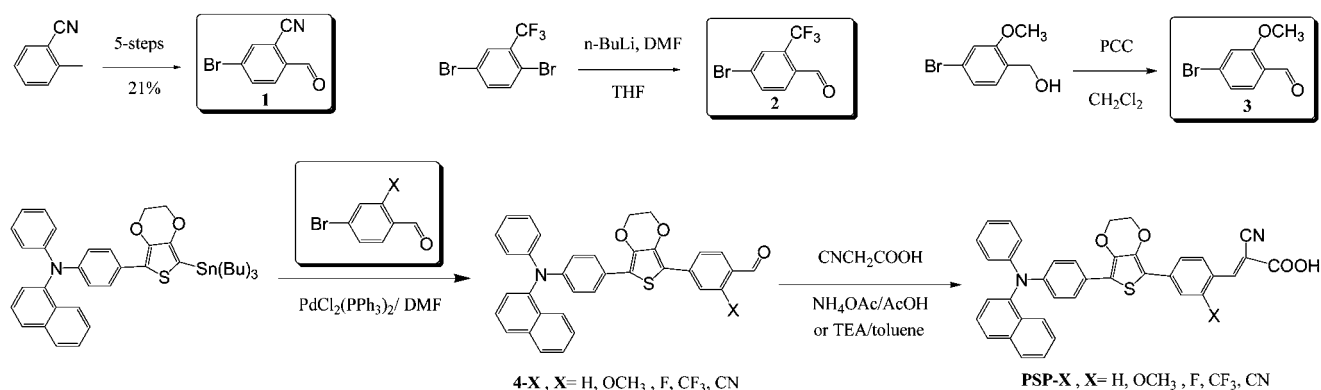
Quantum chemistry computations

The structure of dyes was optimized by using a B3LYP/6-31G* hybrid functional. For the excited states, a time-dependent density functional theory (TDDFT) with the B3LYP functional was employed. All analyses were performed under Q-Chem 3.0 software. The frontier orbital plots of HOMO and LUMO were drawn using Gaussian 03.

Results and discussion

Synthesis of the dyes

Five organic dyes, *i.e.*, PSP-H, PSP-F, PSP-CN, PSP-CF₃ and PSP-OCH₃ were synthesized as outlined in Scheme 1. All compounds are modified at the *ortho*-position of the phenylene group near the A terminal. All syntheses utilized 2-substituted 4-bromobenzaldehydes as the key intermediates. For example, the preparation of 5-bromo-2-formylbenzonitrile (**1**) from *o*-cyano-toluene took 5 steps with a total yield of 21% (ESI[†]).¹⁶ 4-Bromo-2-(trifluoromethyl)benzaldehyde (**2**) was prepared by the formylation of 1,4-dibromo-2-(trifluoromethyl)benzene with *n*-BuLi and DMF. 4-Bromo-2-methoxybenzaldehyde (**3**) was made from (4-bromo-2-methoxy)phenylmethanol by oxidation with pyridinium chlorochromate.¹⁷ The presence of a formyl group in these compounds was verified using ¹H NMR by a downfield signal at δ 10.30~10.38 ppm. The donor moiety was synthesized from *N*-phenyl-1-naphthylamine, onto which the third aromatic group was added by a Buchwald–Hartwig coupling reaction with the aid of Pd(OAc)₂.¹⁸ The resulting triarylamine was then attached onto a 3,4-ethylenedioxythiophene (EDOT) group by a Stille coupling reaction. The reaction was repeated again by attaching it to a 2-substituted 4-bromobenzaldehyde to elongate the chain length. The final step was a Knoevenagel condensation between compound **4** and cyanoacetic acid in the presence of ammonium acetate.¹⁹ This procedure was quite successful for all the products except PSP-CN, for which an apparent decarboxylation happened as a side reaction.²⁰ The synthesis of PSP-CN was finally achieved in low yield by using triethylamine as a base under a refluxed temperature in toluene. All products were confirmed by their corresponding spectroscopic characteristics.



Scheme 1 Synthetic routes of organic dyes (**PSP-X**, X = H, OCH₃, F, CF₃, CN).

Absorption spectra

The UV-Vis absorption spectra of organic dyes in THF solution are displayed in Fig. 1 and the parameters are listed in Table 1. Each of these compounds exhibits three major absorption bands, appearing at 250–260 nm, 330–340 nm, and 440–460 nm, respectively. The first two bands were assigned to localized aromatic π - π^* transitions, and the last one to a charge-transfer (CT) transition. The high intensity of this band is well-correlated with the large value of oscillator strength, which was calculated by a TDDFT/B3LYP modelling study (Table 1). The molar extinction coefficients of both **PSP-H** and **PSP-OCH₃** were quite high, *e.g.* exceeding $4 \times 10^4 \text{ M}^{-1} \text{ cm}^{-1}$ (Fig. 1), while those

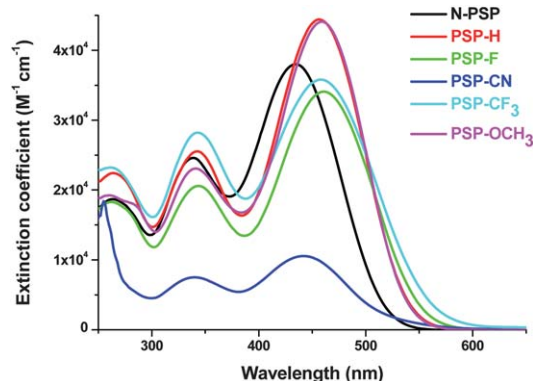


Fig. 1 Absorption spectra of organic dyes in THF.

possessing electron withdrawing groups, *i.e.*, **PSP-F** and **PSP-CF₃**, displayed slightly lower values. It is noteworthy that compound **PSP-CN** exhibited the lowest absorptivity ($\epsilon = 1.06 \times 10^4 \text{ M}^{-1} \text{ cm}^{-1}$), although its longest wavelength tailed to a region comparable to those of **PSP-F** and **PSP-CF₃**. A longer wavelength absorption is favorable to the performance of DSSCs, as more photons with lower energy can be harvested.

The absorption spectra of all dyes on the surface of TiO₂ is shown in Fig. 2. All spectra were blue-shifted about 30–36 nm with respect to those in the solution, except **PSP-CN** which seemed to be red-shifted. The blue-shift on TiO₂ is a common

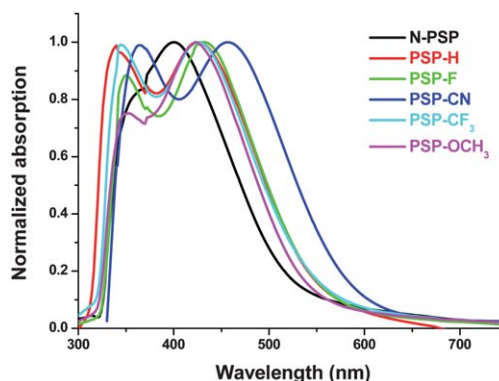


Fig. 2 Absorption spectra of organic dyes adsorbed on TiO₂. The spectra were subtracted from that of pure TiO₂, while the peak minima at *ca.* 300 nm was assumed to be zero.

Table 1 Calculated (TDDFT/B3LYP), absorption, and electrochemical parameters for organic dyes^a

Dye	HOMO/LUMO ^b (eV)	Band gap ^b	<i>f</i> ^b	λ_{abs}^c (nm)/(ϵ ($\text{M}^{-1} \text{ cm}^{-1}$))	λ_{abs} (nm) on TiO ₂	<i>E</i> ₀₋₀ (eV)	<i>E</i> _{ox} ^d (V)	<i>E</i> _{LUMO} ^e (V)
N-PSP	-5.12/-2.63	2.49	0.77	434(37700)	400	2.52	0.82	-1.70
PSP-H	-4.96/-2.47	2.28	0.89	456(42300)	426	2.39	0.71	-1.68
PSP-F	-5.02/-2.55	2.25	0.88	460(34000)	430	2.40	0.72	-1.68
PSP-CN	-5.10/-2.84	2.06	0.72	442(10600)	457	2.36	0.75	-1.61
PSP-CF ₃	-5.02/-2.69	2.13	0.84	458(35800)	426	2.35	0.72	-1.63
PSP-OCH ₃	-4.96/-2.36	2.37	0.99	458(41900)	422	2.39	0.67	-1.72

^a *f*: Oscillator Strength for the lowest energy transition; ϵ : absorption coefficient; *E*_{ox}: oxidation potential; *E*₀₋₀: 0–0 transition energy measured at the intersection of absorption and emission spectra; *J*_{sc}: short-circuit photocurrent density; *V*_{oc}: open-circuit photovoltage; FF: fill factor; η : total power conversion efficiency. ^b TDDFT/B3LYP calculated values. ^c Absorption in THF. ^d Oxidation potential in THF (10^{-3} M) containing 0.1 M (n-C₄H₉)₄NPF₆ with a scan rate 100 mV s^{-1} (vs. NHE). ^e *E*_{LUMO} was calculated by *E*_{ox} – *E*₀₋₀.

phenomenon for most organic dyes, that is regarded as the result of a strong interaction between the dye and the semiconductor surface. A similar trend has been demonstrated while the dyes were deprotonated in the presence of base. Upon deprotonation the electron density in the cyanoacrylate moiety is increased so that the energy level of the LUMO is elevated, consequently the band gap of CT transition is enlarged. However, such an effect is partially annihilated by the presence of a CN group at the *ortho*-position across a phenyl ring, which attracts the extra electron density from the cyanoacrylate through an efficient π -conjugation (Fig. 4).

Electrochemical properties

The oxidation potentials (E_{ox}), corresponding to the HOMO level of dyes, were measured by cyclic voltammetry (CV) in THF solutions, and the results were shown in Fig. 3 and Table 1. The

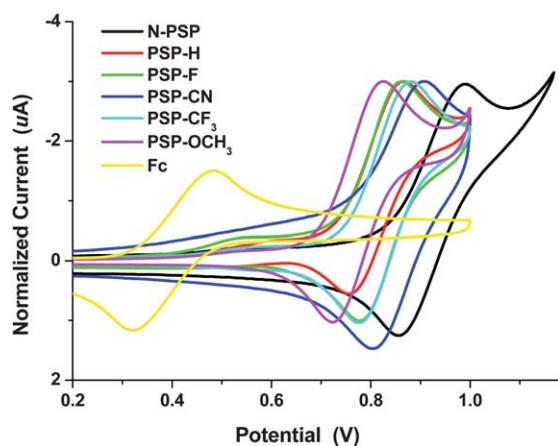


Fig. 3 Oxidative voltammograms of PSP-series organic dyes.

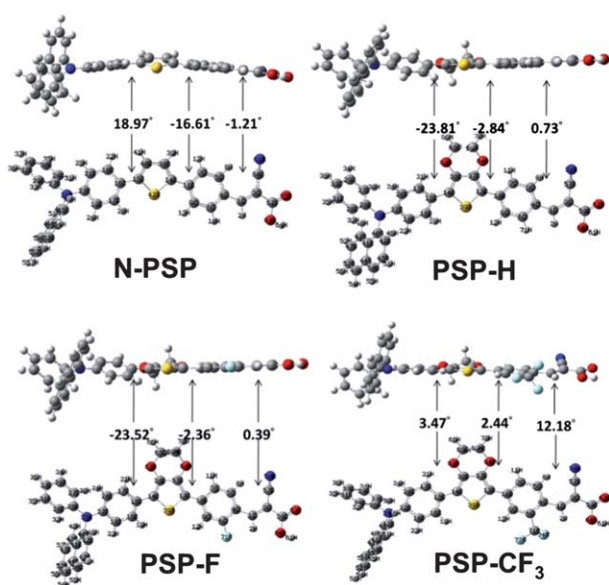


Fig. 4 The optimized structure by TDDFT on B3LYP/6-31G* of N-PSP, PSP-H, PSP-F, and PSP-CF₃.

introduction of an electron-withdrawing group in π -bridge lowered the HOMO level, thus increased the oxidation potential. The potential energy of ionization decreased slightly in the order of **PSP-CN** (0.75) > **PSP-F** (0.72) \approx **PSP-CF₃** (0.72) > **PSP-H** (0.71) > **PSP-OCH₃** (0.67). The HOMO levels thus obtained were within the range 0.75~0.67 eV, which were sufficiently lower than that of electrolyte pair I⁻/I₃⁻ (*ca.* 0.40 V), thus ensured a smooth electron flow from the electrolyte to the dyes. The LUMO levels were estimated by the values of E_{ox} and the 0-0 band gaps, which was estimated at the intersection of absorption and emission spectra. A trend appeared as **PSP-CN** (-1.61) > **PSP-CF₃** (-1.63) > **PSP-H** (-1.68) \approx **PSP-F** (-1.68) > **N-PSP** (-1.70) > **PSP-OCH₃** (-1.72). All these levels were considerably higher than the conductive band level of TiO₂ (*ca.* -0.5 V).

Computational analysis

The structures of the dyes were analyzed using a B3LYP/6-31G* hybrid functional for full geometrical optimization. In the ground state all compounds possess a nearly co-planar conformation to achieve a maximal extent of π -delocalization. Compared to the parent structure of N-PSP, the addition of a dioxane ring in the EDOT moiety did not increase the dihedral angle between the two adjacent aryl groups (Fig. 4). The EDOT moieties may have a function of preventing the formation of aggregates on the surface of TiO₂.²¹

The charge distribution in the frontier molecular orbitals are depicted in Fig. 5. As shown in the graphs, the HOMO level is localized mostly at the triarylamine (D) moiety, while the LUMO is mostly at the cyanoacrylic acid (A). The electron distributions of both D and A are heavily coupled with the orbitals in the central triarylene bridge (B). The geometry of the bridges must have a critical influence on the transition probability of photoexcitation. The calculated potential energy levels of HOMOs and LUMOs compared well with the experimental values of E_{ox} and

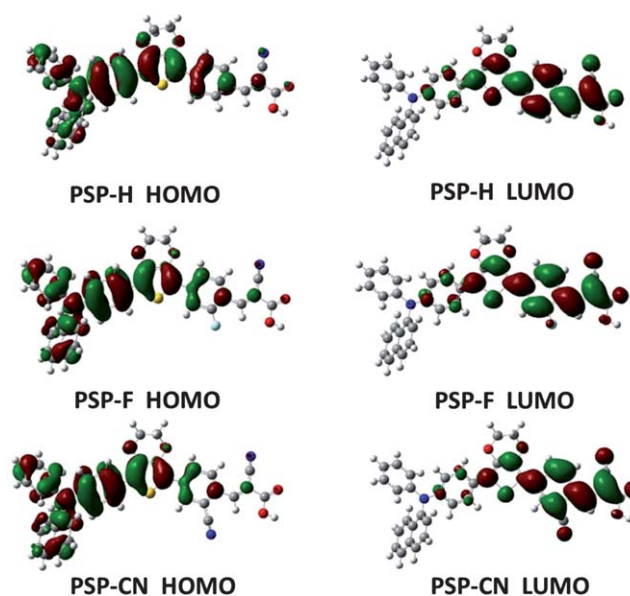


Fig. 5 Computed frontier orbitals of dyes. The left graphs are the HOMOs, and the right ones are the LUMOs.

E_{LUMO} estimated by CV. The electron-withdrawing substituents on the acceptor moiety should have an effect of stabilizing the charge-separated species upon photo-excitation. As indicated in Fig. 5, the electron density on the LUMOs of **PSP-F** and **PSP-CN** can spread more widely onto the substituents, *cf.* that of **PSP-H**.

The transition probability was estimated by time-dependent density functional theory (TDDFT) with the B3LYP functional, and the calculated oscillator strength (f) is shown in Table 1. The f values for the lowest energy transitions, *i.e.*, the CT transitions, are all relatively high, *e.g.*, ranging from 0.72~0.99. The results are consistent with the absorptivity measured in solutions, except for **PSP-CN**. The absorption coefficient (ϵ) of all dyes measured by experiment was significantly lower than expected (Fig. 1 and Table 1).

Photovoltaic performance of DSSCs

The photocurrent–voltage (J – V) plots of DSSCs fabricated with these dyes, along with that of N719 for comparison, are shown in Fig. 6. The detailed parameters, *i.e.*, short circuit current (J_{sc}), open-circuit photovoltage (V_{oc}), fill factor (ff), and solar-to-electrical photocurrent density (η) measured under AM 1.5 solar light (100 mW cm^{-2}) are summarized in Table 2. All dyes with an EDOT group exhibit a higher values of J_{sc} ($15.2\sim 17.0$) than the parent compound **N-PSP** without it ($J_{\text{sc}} = 15.0$), presumably due to a more extended delocalization. The absorption range of the former is apparently longer than that of the latter (Fig. 2). The only exception is **PSP-CN**, which yielded a low value for the short circuit current, *i.e.*, 8.3 mA cm^{-2} only about half of the others. It was mainly ascribed to its low molar absorptivity extinction coefficient, as indicated in Fig. 1 and Table 1. All the new dyes, except **PSP-CN**, performed better than **N-PSP** exhibiting a higher quantum efficiency.

It is known that reducing the amount of dark current can retard charge recombination, thus increase the efficiency of the solar cells.²² The dark currents were found to be in the order of **PSP-CN** > **PSP-OCH₃** > **PSP-H** > **PSP-F** > **PSP-CF₃** as shown in the bottom of Fig. 6. The amount of open current voltage (V_{oc}) can be benefited by reducing the charge

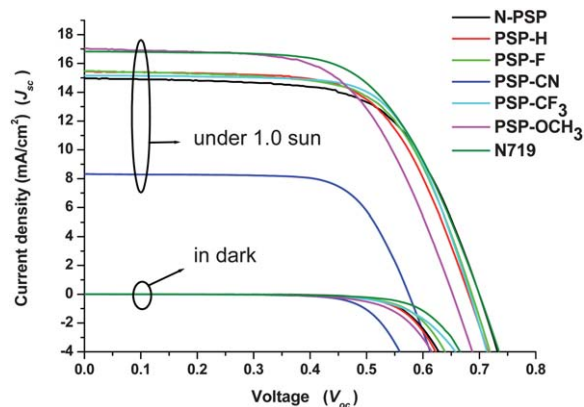


Fig. 6 J – V curves of the DSSC devices made with the dyes. The plots in the upper section were measured under the light intensity of 1.0 sun. The plots in the bottom half were taken in the dark.

Table 2 Photovoltaic parameters for DSSCs of **PSP-series**^a

Dye	J_{sc} (mA cm^{-2})	V_{oc} (V)	ff	η^c (%)
N-PSP	14.96	0.70	0.64	6.71
PSP-H	15.44	0.68	0.64	6.76
PSP-F	15.48	0.69	0.65	6.87
PSP-CN	8.32	0.58	0.70	3.37
PSP-CF₃	15.16	0.68	0.68	7.00
PSP-OCH₃	17.04	0.65	0.61	6.72
N719	16.84	0.705	0.62	7.32

^a Performance of DSSC measured in a 0.25 cm^2 working area on a FTO ($8\Omega/\text{square}$) substrate.

recombination rate in the nanocrystallite/dye/redox electrolyte interface. The order of open current voltages matched with the trend of reducing dark current, *i.e.*, **PSP-CN** (0.58) < **PSP-OCH₃** (0.65) < **PSP-H** = **PSP-F** (0.68) < **PSP-CF₃** (0.69). It is noteworthy that the fill factor increased with the strength of the electron-withdrawing ability, particularly in the cases of **PSP-CN** and **PSP-CF₃** ($ff = 0.68\sim 0.70$).

Among all the devices, except **PSP-CN**, the ones with strong electron-withdrawing groups performed the best, *e.g.*, the solar-to-electricity conversion efficiency for **PSP-F** was 6.87%, and that for **PSP-CF₃** was 7.00%. Their IPCE values in the region of 380~620 nm were all >50% (Fig. 7). For the abnormal behaviour of **PSP-CN**, it may be compared to previous reports revealing that a strong electron-withdrawing cyano group located at the proximity of the acceptor might jeopardise the injection of electrons toward the conducting electrode.²⁰ The best performance in this work was observed for the device made with **PSP-CF₃**, which exhibited a J_{sc} value 15.16 mA cm^{-2} , V_{oc} value of 0.68 V, and ff value of 0.68. The overall conversion efficiency (η) was estimated to be 7.0%, which was quite comparable to the well-known ruthenium complex **N-719**. The incident photon to current conversion efficiency (IPCE) was higher than 70% in the range 420~540 nm. It is worth noting that in a recent report, Chou and Chi has found that adding a fluorine substituent at the *meta* position to the cyanoacrylate can induce a profound effect on the quantum efficiency of DSSC.^{12b} In our comparative analysis, the trifluoromethyl substituent (**PSP-CF₃**) works even better than the fluorine (**PSP-F**).

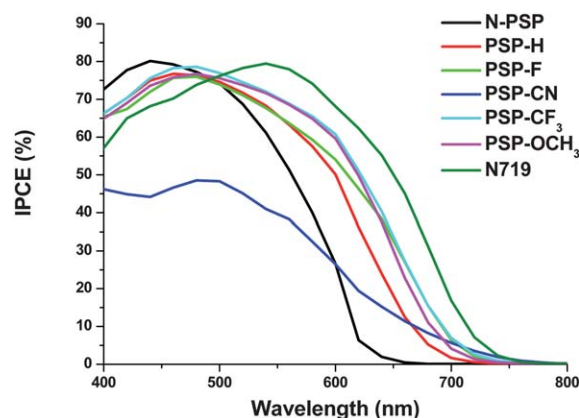


Fig. 7 IPCE curves of **PSP-series** organic dyes.

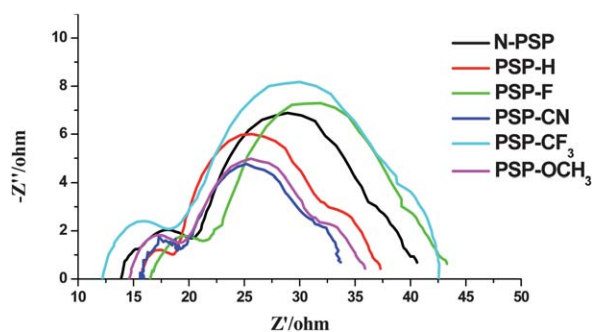


Fig. 8 EIS Nyquist plots of electrochemical impedance of the DSSCs made with the dyes at -0.73 V bias in the dark.

Electrochemical impedance spectroscopy

Electrochemical impedance spectroscopy (EIS) analysis was performed to further elucidate the photovoltaic properties. Fig. 8 shows the electrochemical impedance spectra for the DSSCs made with TiO_2 electrodes, dipped with the **PSP**-series sensitizers under a forward bias of -0.73 V in the dark. Three semicircles were observed in the Nyquist plots. The first one is attributed to the high-frequency peak ($>10^2$ Hz) is ascribed to the charge-transfer process at the interfaces between the redox couple and the platinized counter electrode. The middle-frequency peak (in the 10–100 Hz region) is related to the transport process of the injected electrons at the interfaces between TiO_2 and the electrolyte/dye, and the low frequency one (<1 Hz) is associated with the Nernst diffusion of I_3^- within the electrolyte (EIS Bode plots in ESI).²³

The charge recombination resistance at the TiO_2 surface (R_{rec}), it can be deduced by fitting curves from a range of intermediate frequencies using Z-view software. It is related to the charge recombination rate, e.g., a smaller R_{rec} indicates a faster charge recombination and therefore a larger dark current (Fig. 6). The radius of the biggest semicircle increases in the order **PSP-CN** (11.3 ohm) $<$ **PSP-OCH₃** (12.0 ohm) $<$ **PSP-H** (13.3 ohm) $<$ **PSP-F** (18.0 ohm) $<$ **PSP-CF₃** (20.7 ohm). This trend appears to be consistent with both the lower V_{oc} values of **PSP-CN** (0.58 V) and **PSP-OCH₃** (0.65 V), as well as the higher values of **PSP-F** (0.69 V) and **PSP-CF₃** (0.68 V). It seems reasonable to conclude that the better performance of the latter can be ascribed to a reduced rate of charge recombination, which led to higher values of V_{oc} .

Conclusions

The presence of a substituent on the phenyl group *ortho* to the cyanoacrylate acceptor of the dyes can effectively elongate the absorption wavelength. A wider wavelength of absorption is favourable to the light-harvesting efficiency of DSSCs. The compound **PSP-OCH₃** thus exhibited the highest J_{sc} value of all. However, an electron-withdrawing substituent was capable of stabilizing the negative charge developed in the CT state, and thus reduced the rate of charge recombination. Such an effect can be evidenced by the high V_{oc} values of both compounds **PSP-F** and **PSP-CF₃**. A combined effect of the above two factors resulted in the highest ff value for **PSP-CF₃**, which yielded the best performance with a η value 7.0%. The replacement of the

central thiophene group of **N-PSP** by an EDOT group have also promoted slightly the performance of devices, presumably due to the prevention of aggregation on the surface of TiO_2 .

An exception was found for compound **PSP-CN**, which exhibited a low absorption on the CT transition which led to a small value of J_{sc} (8.32). Its overall quantum efficiency was found to be 3.37% only, despite its high ff factor (0.70). The low absorptivity may be ascribed to the electronic configuration in the ground state, which does not favour a CT transition from the D (triarylamine) to A (cyanoacrylate). Shifting the CN group to other site of the phenyl group in future designs may alter the selection rule of the CT transition.

Acknowledgements

Financial supports from the National Science Council of Taiwan and Academia Sinica are gratefully acknowledged. Special thanks to Professor C.-P. Hsu at the Institute of Chemistry for her assistance on the quantum chemistry computations.

References

- B. O'Regan and M. Grätzel, *Nature*, 1999, **352**, 737.
- (a) M. K. Nazeeruddin, A. Key, I. Rodicio, R. Humphry-Baker, E. Müller, P. Liska, N. Vlachopoulos and M. Grätzel, *J. Am. Chem. Soc.*, 1993, **115**, 6382; (b) M. K. Nazeeruddin, S. M. Zakeeruddin, R. Humphry-Baker, M. Jirousek, P. Liska, N. Vlachopoulos, V. Shklover, C. H. Fischer and M. Grätzel, *Inorg. Chem.*, 1999, **38**, 6298; (c) M. K. Nazeeruddin, P. Péchy, T. Renouard, S. M. Zakeeruddin, R. Humphry-Baker, P. Comte, P. Liska, L. Cevey, E. Costa, V. Shklover, L. Spiccia, G. B. Deacon, C. A. Bignozzi and M. Grätzel, *J. Am. Chem. Soc.*, 2001, **123**, 1613; (d) M. Grätzel, *Inorg. Chem.*, 2005, **44**, 6841.
- (a) Z.-S. Wang, Y. Cui, K. Hara, Y. Dan-oh, C. Kasada and A. Shinpo, *Adv. Mater.*, 2007, **19**, 1138; (b) K. Hara, K. Miyamoto, Y. Abe and M. Yanagida, *J. Phys. Chem. B*, 2005, **109**, 23776.
- D. Kuang, S. Uchida, R. Humphry-Baker, S. M. Zakeeruddin and M. Grätzel, *Angew. Chem., Int. Ed.*, 2008, **47**, 1923.
- (a) A. Ehret, L. Stuhl and M. T. Spitler, *J. Phys. Chem. B*, 2001, **105**, 9960; (b) K. Sayama, K. Hara, Y. Ohga, A. Shinpou, S. Suga and H. Arakawa, *New J. Chem.*, 2001, **25**, 200.
- K. Sayama, S. Tsukagoshi, K. Hara, Y. Ohga, A. Shinpou, Y. Abe, S. Suga and H. Arakawa, *J. Phys. Chem. B*, 2002, **106**, 1363.
- (a) Q.-H. Yao, L. Shan, F.-Y. Li, D.-D. Yin and C.-H. Huang, *New J. Chem.*, 2003, **27**, 1277; (b) Q.-H. Yao, F.-S. Meng, F.-Y. Li, H. Tian and C.-H. Huang, *J. Mater. Chem.*, 2003, **13**, 1048.
- (a) S. Ferrere and B. A. Gregg, *New J. Chem.*, 2002, **26**, 1155; (b) T. Edvinsson, C. Li, N. Pschirer, J. Schöneboom, F. Eickemeyer, R. Sens, G. Boschloo, A. Herrmann, K. Müllen and A. Hagfeldt, *J. Phys. Chem. C*, 2007, **111**, 15137; (c) Y. Shibano, T. Umeyama, Y. Matano and H. Imahori, *Org. Lett.*, 2007, **9**, 1971; (d) J. Fortage, M. Séverac, C. H. Rassin, Y. Pellegrin, E. Blart and F. Odobel, *J. Photochem. Photobiol., A*, 2008, **197**, 156; (e) H. Imahori, T. Umeyama and S. Ito, *Acc. Chem. Res.*, 2009, **42**, 1809.
- (a) S. Ko, H. Choi, M.-S. Kang, H. Hwang, H. Ji, J. Kim, J. Ko and Y. Kang, *J. Mater. Chem.*, 2010, **20**, 2391; (b) L.-Y. Lin, C.-H. Tsai, K.-T. Wong, T.-W. Huang, L. Hsieh, S.-H. Liu, H.-W. Lin, C.-C. Wu, S.-H. Chou, S.-H. Chen and A.-I. Tsai, *J. Org. Chem.*, 2010, **75**, 4778.
- (a) S. Eu, S. Hayashi, T. Umeyama, A. Oguro, M. Kawasaki, N. Kadota, Y. Matano and H. Imahori, *J. Phys. Chem. C*, 2007, **111**, 3528; (b) J.-J. Cid, J.-H. Yum, S.-R. Jang, M. K. Nazeeruddin, E. Martínez-Ferrero, E. Palomares, J. Ko, M. Grätzel and T. Torres, *Angew. Chem., Int. Ed.*, 2007, **46**, 8358; (c) H.-P. Lu, C.-L. Mai, C.-Y. Tsia, S.-J. Hsu, C.-P. Hsieh, C.-L. Chiu, C.-Y. Yeh and E. W.-G. Diau, *Phys. Chem. Chem. Phys.*, 2009, **11**, 10270; (d) C.-L. Mai, W.-K. Huang, H.-P. Lu, C.-W. Lee, Y.-R. Liang, E. W.-G. Diau and C.-Y. Yeh, *Chem. Commun.*, 2010, **46**, 809.

- 11 (a) Y.-J. Chang and T. J. Chow, *Tetrahedron*, 2009, **65**, 4726; (b) Y.-J. Chang and T. J. Chow, *Tetrahedron*, 2009, **65**, 9626.
- 12 (a) J.-H. Yum, D. P. Hagberg, S.-J. Moon, K. M. Karlsson, T. Marinado, L. Sun, A. Hagfeldt, M. K. Nazeeruddin and M. Grätzel, *Angew. Chem., Int. Ed.*, 2009, **48**, 1576; (b) H. Im, S. Kim, C. Park, S.-H. Jang, C.-J. Kim, K. Kim, N.-G. Park and C. Kim, *Chem. Commun.*, 2010, **46**, 1335; (c) G. Zhang, Y. Bai, R. Li, D. Shi, S. Wenger, S. M. Zakeeruddin, M. Grätzel and P. Wang, *Energy Environ. Sci.*, 2009, **2**, 92; (d) D. P. Hagberg, J.-H. Yum, H. Lee, F. D. Angelis, T. Marinado, K. M. Karlsson, R. Humphry-Baker, L. Sun, A. Hagfeldt, M. Grätzel and M. K. Nazeeruddin, *J. Am. Chem. Soc.*, 2008, **130**, 6259; (e) C. Kim, H. Choi, S. Kim, C. Baik, K. Song, M.-S. Kang, S. O. Kang and J. Ko, *J. Org. Chem.*, 2008, **73**, 7072; (f) M. Xu, R. Li, N. Pootrakulchote, D. Shi, J. Guo, Z. Yi, S. M. Zakeeruddin, M. Grätzel and P. Wang, *J. Phys. Chem. C*, 2008, **112**, 19770; (g) D. Shi, Y. Cao, N. Pootrakulchote, Z. Yi, M. Xu, S. M. Zakeeruddin, M. Grätzel and P. Wang, *J. Phys. Chem. C*, 2008, **112**, 17478; (h) R. Li, X. Lv, D. Shi, D. Zhou, Y. Cheng, G. Zhang and P. Wang, *J. Phys. Chem. C*, 2009, **113**, 7469.
- 13 J. Song, F. Zhang, C. Li, W. Liu, B. Li, Y. Huang and Z. Bo, *J. Phys. Chem. C*, 2009, **113**, 13391.
- 14 (a) W.-H. Liu, I.-C. Wu, C.-H. Lai, C.-H. Lai, P.-T. Chou, Y.-T. Li, C.-L. Chen, Y.-Y. Hsu and Y. Chi, *Chem. Commun.*, 2008, 5152; (b) B.-S. Chen, D.-Y. Chen, C.-L. Chen, C.-W. Hsu, H.-C. Hsu, K.-L. Wu, S.-H. Liu, P.-T. Chou and Y. Chi, *J. Mater. Chem.*, 2011, **21**, 1937.
- 15 W. Zeng, Y. Cao, Yu. Bai, Y. Wang, Y. Shi, Min. Zhang, F. Wang, C. Pan and P. Wang, *Chem. Mater.*, 2010, **22**, 1915.
- 16 C.-L. Li, S.-J. Shieh, S.-C. Lin and R.-S. Liu, *Org. Lett.*, 2003, **5**, 1131.
- 17 M. Dąbrowski, J. Kubicka, S. Luliński and Janusz Serwatowski, *Tetrahedron*, 2005, **61**, 6590.
- 18 S. Urgaonkar, M. Nagarajan and J. G. Verkade, *J. Org. Chem.*, 2003, **68**, 452.
- 19 E. Knoevenagel, *Angew. Chem., Int. Ed. Engl.*, 1922, **35**, 29.
- 20 H. Tian, X. Yang, R. Chen, R. Zhang, A. Hagfeldt and L. Sun, *J. Phys. Chem. C*, 2008, **112**, 11023.
- 21 G. Zhang, H. Bala, Y. Cheng, D. Shi, X. Lv, Q. Yu and P. Wang, *Chem. Commun.*, 2010, 2198.
- 22 W. Wu, J. Yang, J. Hua, J. Tang, L. Zhang, Y. Long and H. Tian, *J. Mater. Chem.*, 2010, **20**, 1772.
- 23 (a) K. R. Justin Thomas, Y.-C. Hsu, J.-T. Lin, K.-M. Lee, K.-C. Ho, C.-H. Lai, Y.-M. Cheng and P. T. Chou, *Chem. Mater.*, 2008, **20**, 1830; (b) Q. Li, L. Lu, C. Zhong, J. Huang, Q. Huang, J. Shi, X. Jin, T. Peng, J. Qin and Z. Li, *Chem.-Eur. J.*, 2009, **15**, 9664; (c) N. Cho, H. Choi, D. Kim, K. Song, M.-S. Kang, S. O. Kang and J. Ko, *Tetrahedron*, 2009, **65**, 6236; (d) J. Tang, J. Hua, W. Wu, J. Li, Z. Jin, Y. Long and H. Tian, *Energy Environ. Sci.*, 2010, **3**, 1736.